Egyptian Journal of Pure and Applied Science

^{99m}Tc-Citrate-gold nanoparticles as a tumor tracer: Synthesis, characterization, radiolabeling and *in-vivo* studies

Basma M. Essa[1*], Maher A. El-Hashash[2], Ahmed A. El-Mohty[1] and Tamer M. Sakr[1]

[1] *Radioactive Isotopes and Generator Department, Hot Labs Center, Egyptian Atomic Energy Authority (EAEA), P.O. Box 13759, Cairo, Egypt.*

[2]*Chemistry Department, Faculty of Science, Ain Shams University, Cairo, Egypt.*

ARTICLE INFO

Article history:
Received 21 February 2018
Accepted 10 March 2019

Keywords:
Gold nanoparticles;
sodium citrate;
technetium-99m;
labeling;
tumor.

ABSTRACT

Targeted drug delivery system can reduce the side effects of high drug concentration by improving drug pharmacokinetics at lower doses. Citrate-AuNPs as a drug delivery system were synthesized via green nanotechnology technique with core size of 10 nm. Citrate-AuNPs were labeled with technetium-99m with radiochemical yield of 85.2 % with good *in-vitro* stability. By studying the biodistribution of [^{99m}Tc]Tc-citrate-AuNPs in solid tumor bearing mice; promising data appeared high uptake and good retention of [^{99m}Tc] Tc-citrate-AuNPs in tumor tissues. As a result, the newly nano-platform showed high tumor uptake, which affords potential radiopharmaceutical that could be used as a good tumor imaging probe.

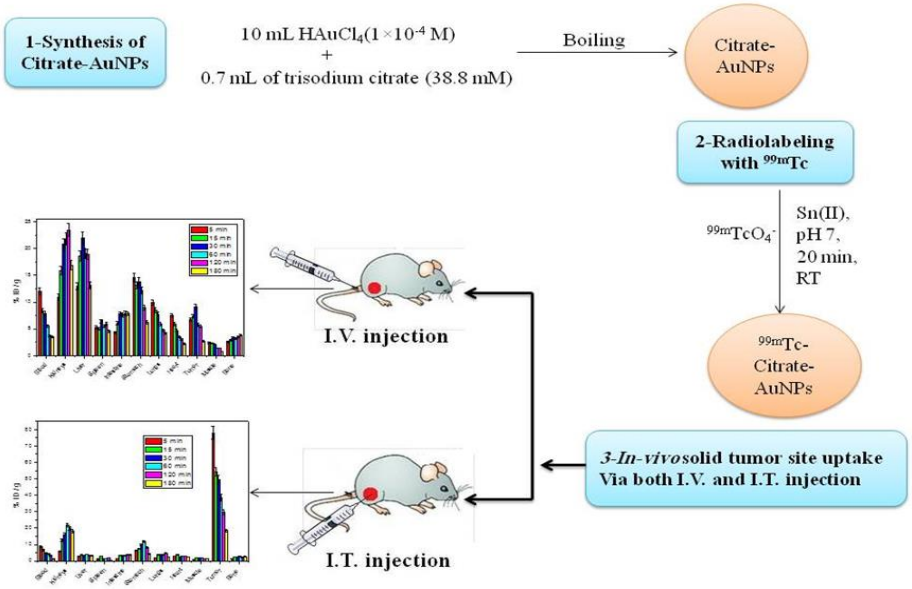

Introduction

Cancer is already a major disease of the aging so plenty of works were done to overcome this ghost of death. Early detection of cancer is an important aspect in treatment [1]. Nanotechnology is one of the possible methods to enhance cancer imaging efficacy with minimal side effect using targeted drug delivery technique [2]. It introduces exceptional advantages in cancers treatment because it showed some promise results for delivering NP-targeted agents to tumors [3].

Tumor targeted delivery-based nanotechnology uses materials sized between 1 and 100 nm [4]. Among different metal nanoparticles that have been widely used, gold nanoparticles (AuNPs) are well documented due to many characteristics such as: i) biologically non-reactive, ii) tailored with different sizes easily, iii) have surface plasmonic characteristics, iv) immobilize various biomolecules which make it stable under various conditions [5]. All these appealing properties of AuNPs make it suitable for use various biological applications including biomedicine, diagnosis and cancer therapy [6].

* Corresponding author.
E-mail address: basmamohamed24@yahoo.com

Green nanotechnology was developed to overcome the drawbacks of the chemical methods that used in the synthesis of nanoparticles [7]. Citric acid is a naturally occurring tricarboxylic acid, is a major substrate for energy generation in most cells [8]. It is an essential donor for protein acetylation and an intermediate in the tricarboxylic acid (TCA) (or mitochondrial Krebs' cycle). Citrate is used for fatty acid synthesis, which increased in cancer cells [8]. It was suggested that citrate may play a role in cancer biology [9] and it inhibits tumor cell proliferation in multiple tumor lines and it was suggested that it can inhibit tumor growth [10].

Radiolabeled nanoparticles are one of the various contrast agents for different imaging modalities which were constructed *via* nanotechnology [11-13]. Radioisotopes have an integral part of the medical applications field especially in diagnostic applications [14]. Technetium-99m was considered as a trump card between all radioisotopes due to its nearly ideal properties (suitable physical half-life, appropriate energy, cheap and readily available) [15-17]. This work aims to synthesize citrate-AuNPs label with ^{99m}Tc for tumor imaging.

Subjects and Methods

Chemicals

Chloroauric acid, trisodium citrate, absolute ethanol, ammonia solution and acetone were purchased from Sigma Aldrich, St. Louis, USA. Stannous chloride dihydrate ($SnCl_2.2H_2O$) was purchased from (Merck, Darmstadt, Germany). Technetium-99m (^{99m}Tc) ($T_{1/2}$=6h, Eγ=140 keV) was obtained from a ^{99}Mo-^{99m}Tc generator (RPF, Egyptian Atomic Energy Authority, Egypt). All solutions were prepared using deionized water.

Instrumentation

The particles size was analysed by transmission electron microscope (TEM) using JEOL 2000FX TEM operated at 200 kV (Ted Pella, Redding, CA, USA). The hydrodynamic particles size distribution in the colloid was measured using a zetasizer (Malvern Zetasizer Nano ZS 90, ATA Scientific Pty. Ltd., Australia), which is based on a dynamic light scattering technique. Zeta potential was determined using Photo correlation spectrometer (PCS) Brookhaven 90 plus (Zetasizer Nano™, Beckman Coulter, Miami, FL, USA). Radioactivity measurements were done in a NaI(TI) well-type gamma counter (Scale Ratemeter SR7 model (Nuclear enterprises LTD, Edinburg, TX, USA).

Animals

The biodistribution was evaluated in Swiss Albino mice (20 – 25 g).

Synthesis of citrate gold nanoparticles (citrate-AuNPs)

10 mL of chloroauric acid solution (1×10^{-4} M) were heated to the boiling point then 0.7 mL of trisodium citrate solution (38.8 mM) were added dropwise under vigorous mechanical stirring for 30 minutes [18].

Complexation of citrate-AuNPs with technetium-99m

The generator was eluted during all experiments every 24 hours. ^{99m}Tc-labeling parameters for citrate-AuNPs complex formation were optimized *via* a series of experiments. In 5 mL reaction volume, all reaction conditions were studied in different ranges. Sn(II) amount (2 - 20 µg), pH (6 - 10), volume of citrate-AuNPs (0.5 - 3 mL) and reaction time (5 - 360 min).

Radiochemical yield of [^{99m}Tc] Tc-citrate-AuNPs complex

The radiochemical yield of [^{99m}Tc]Tc-citrate-AuNPs complex was evaluated by ascending paper chromatography (Whatman No.1, Whatman International Ltd, Maidstone, Kent, UK) using two mobile phases acetone and water: ethanol: ammonia mixture (5:2:1, v/v/v) as developing solvents. Strips of paper chromatography of 1 cm wide and 13 cm long marked from lower end at a distance of 2 cm and lined into sections (1 cm each) up to 10 cm. Acetone was used to determine the percent of free $^{99m}TcO_4^-$ at R_f = 1; while mixture used to determine the percent of reduced hydrolyzed-^{99m}Tc colloid at R_f = 0. After completing the developing process, the strips were dried, cut into 1 cm pieces and counted using the γ-ray scintillation counter. The percent of [^{99m}Tc]Tc-citrate-AuNPs complex was calculated as follows:

Labeling yield = 100 - (% free $^{99m}TcO_4^-$ + % reduced hydrolyzed ^{99m}Tc colloid).

In-vitro stability study in saline and human serum

Exactly 0.2 mL of the [^{99m}Tc]Tc-citrate-AuNPs was added to 1.8 mL 0.9 % saline or human serum then incubated at 37ºC for 24 h. The radiochemical yield was checked at 0, 3, 6, 12 and 24 h of incubation period.

In-vitro cytotoxicity study

In-vitro cell viability assay was carried out against MRC-5 (Normal human lung fibroblast cells) using MTT assay. The cells were incubated in the presence of various concentrations of citrate-AuNPs at 37ºC in a humidified atmosphere with 5 % CO_2 for 24 h.

Biodistribution studies

The experiment was done according to the approved protocol of the study by the Egyptian Atomic Energy Authority (EAEA) animal ethics committee (EAEA/2017/167) where principles of the Declaration of Helsinki as amended in Seoul 2008 for humans, and the European Community guidelines for the use of experimental animals, were followed.

Tumor induction in mice

Ehrlich ascites carcinoma as a parent tumor line was withdrawn from a donor female Albino mouse and diluted with physiological saline solution. 0.2 mL of the solution was then intramuscularly injected in the right thigh producing a solid tumor after 4 - 6 days.

Biodistribution

The biodistribution studies of the [^{99m}Tc]Tc-citrate-AuNPs were performed in three groups of mice "A" (normal mice), "B" and "C" (solid tumor bearing mice).

Each group was carried out on 18 mice (six points and each point carried out on 3 mice). [^{99m}Tc]Tc-citrate-AuNPs was injected intravenously (I.V.) in group A and C, and intra tumor (I.T.) in group "B". The animals were anaesthetized using chloroform, then weighed and sacrificed at different time intervals (5, 15, 30, 60, 120 and 180 min. post injection). All organs and tissues were separated and washed with physiological saline then weighed. Samples from blood, bone and muscle were collected and taken as 7, 10 and 40 % of the total body weight, respectively. The radioactivity of each organ was measured in a well type γ-counter NaI(Tl). The target to non-target ratio (T/NT) (tumor muscles to normal muscles) was calculated. The results obtained were expressed as percent dose per gram.

Results

Characterization of citrate-AuNPs

The synthesized colloidal gold using tri sodium citrate was well characterized by both dynamic light scattering (DLS) to determine its hydrodynamic diameter and TEM for core size determination. Hydrodynamic diameter was 21.4 nm **Fig. 1a** and core size diameter was 10 nm **Fig. 1b**, also zeta potential for citrate-AuNPs was measured and equal to -11.8 mV **Fig. 2.**

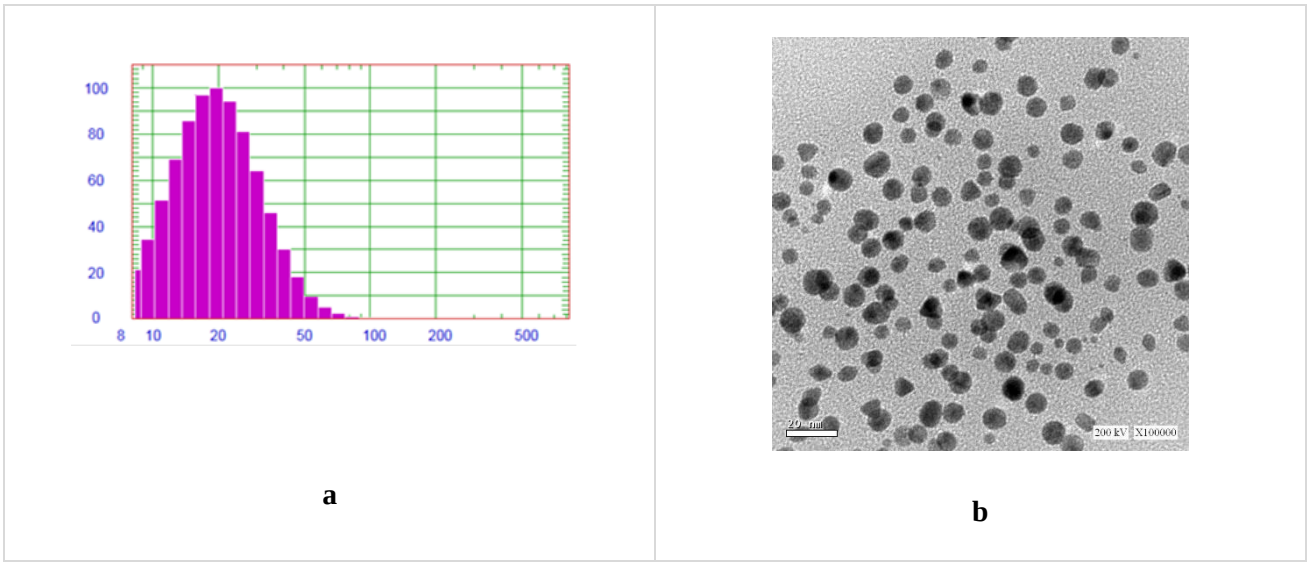

Fig. 1: Citrate-AuNPs size: **a-** The size distribution histogram. **b-** TEM image of citrate-AuNPs.

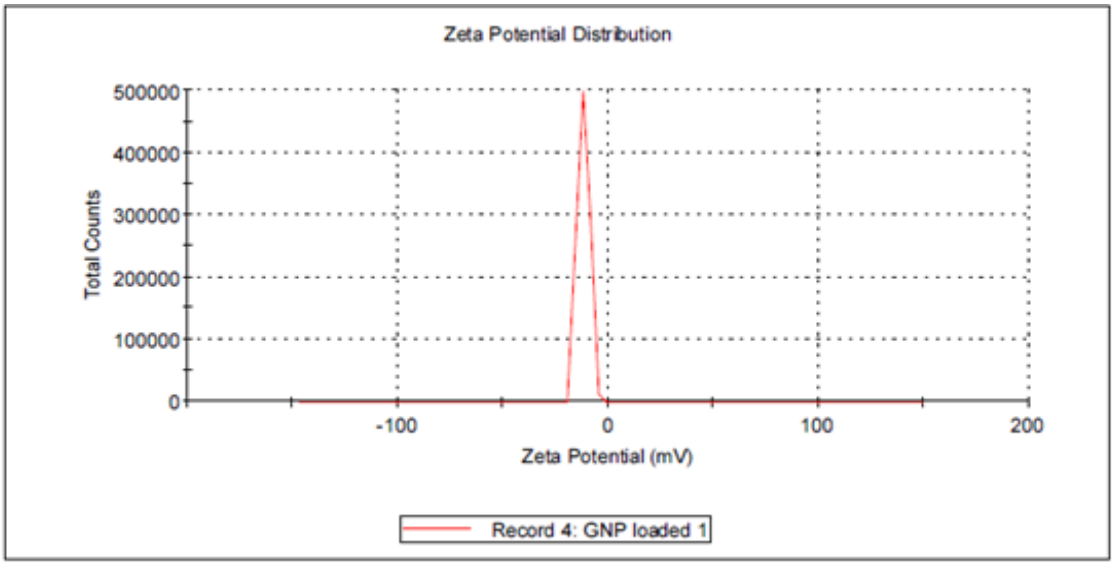

Fig. 2: Zeta potential distribution of citrate-AuNPs.

Radiolabeling of citrate-AuNPs

The maximum radiochemical yield of 85.2 % was obtained by using an efficient amount of Sn(II) (10 µg) using 1 mL of citrate-AuNPs solutions at pH 7 after 20 min at room temperature **Fig. 3(a-d)**.

Physiological *in-vitro* stability

In-vitro stability study of the [^{99m}Tc]Tc-citrate-AuNPs in both saline and human serum **Fig. 4** indicates that [^{99m}Tc]Tc-citrate-AuNPs complex was stable under physiological conditions, where only 1.1 % of the complex was lost after 6 h and about 3 % decrease in the radiochemical yield after 24 h incubation period.

***In-vitro* cytotoxicity study**

The *in-vitro* cytotoxicity evaluation of citrate-AuNPs against MRC-5 (Normal human lung fibroblast cells) indicated that IC50 was 1.7 ± 0.18 µl/100µl **Fig. 5**.

Biodistribution studies

[^{99m}Tc]Tc-citrate-AuNPs were injected intravenously (I.V.) **Fig. 6a** in normal mice (group A) and the results revealed that the maximum radioactivity uptake in the liver, spleen and lungs were 23.39, 7.02 and 10.53 % ID/g at 120, 30 and 5 min p.i., respectively. The highest concentration of [^{99m}Tc]Tc-citrate-AuNPs in blood pool was 12.98 % ID/g at 5 min p.i. and decreased gradually reached to 3.47 % ID/g at 180 min p.i. The radioactivity accumulation in kidney was 19.73 % ID/g at 30 min p.i. and decreased with time. The biodistribution study in group B after I.T. injection **Fig. 6b** demonstrated that most of the radioactivity accumulation was noticed in tumor site reaching to 77.86 at 5 min and still around 50 % after 30 min p.i. For group C **Fig. 6c** the maximum radioactivity accumulation in tumor was achieved at 30 min p.i. which reached to 4.35 expressed as target to non-target ratio (T/NT) **Fig. 6d** and sustained high (3.9) at 120 min p.i.

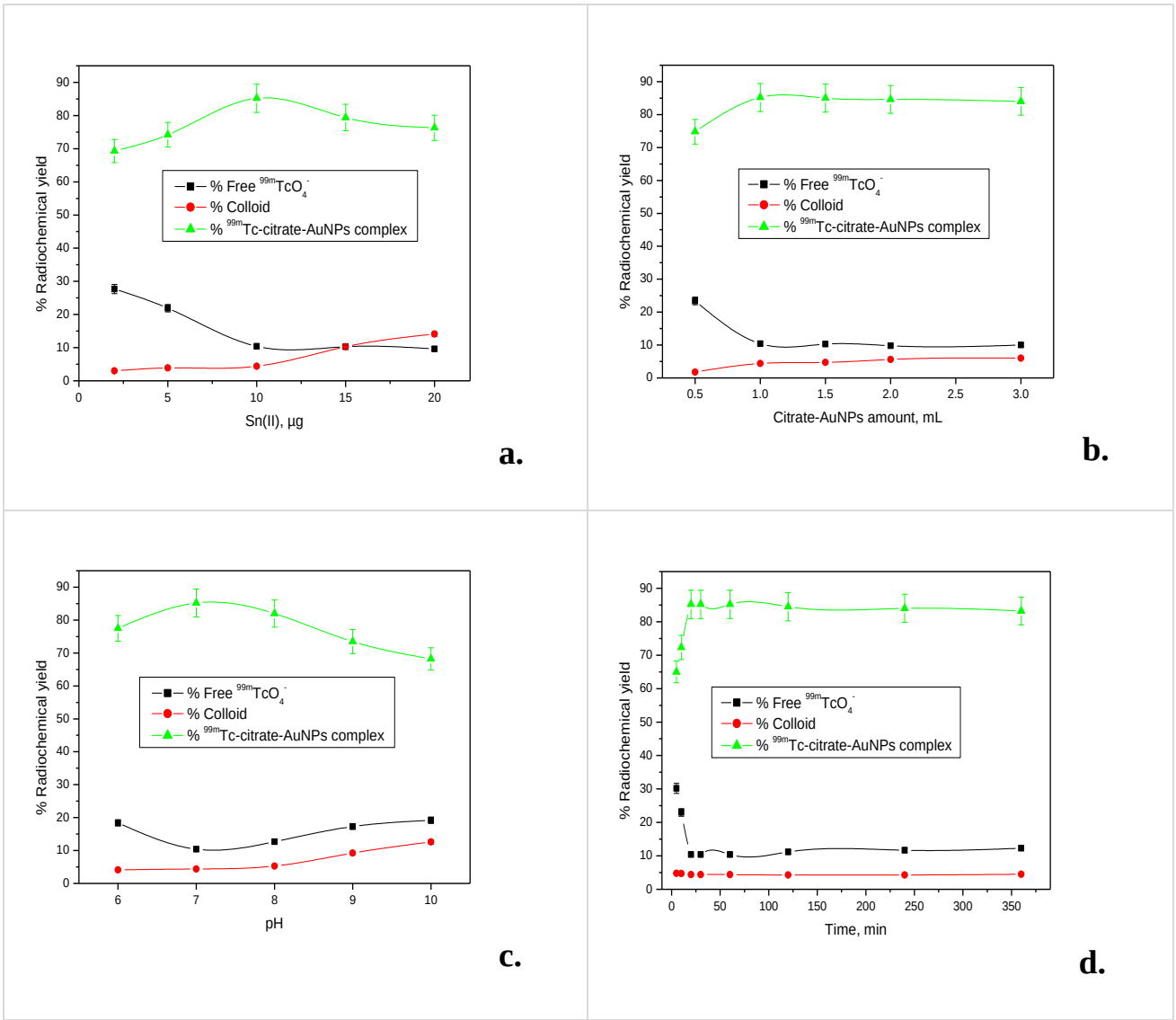

Fig. 3: Radiochemical yield of [^{99m}Tc]Tc-citrate-AuNPs as a function of: **a-** reducing agent amount, **b-** substrate content, **c-** pH, **d-** reaction time.

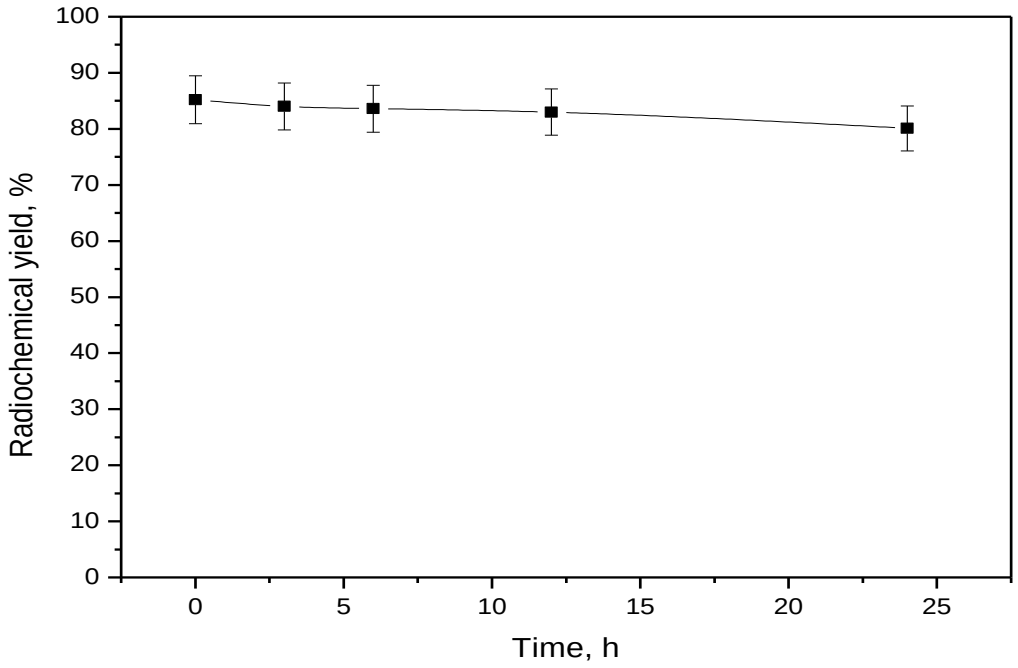

Fig. 4: Stability of [^{99m}Tc]Tc-citrate-AuNPs in saline / human serum at 37ºC followed in time.

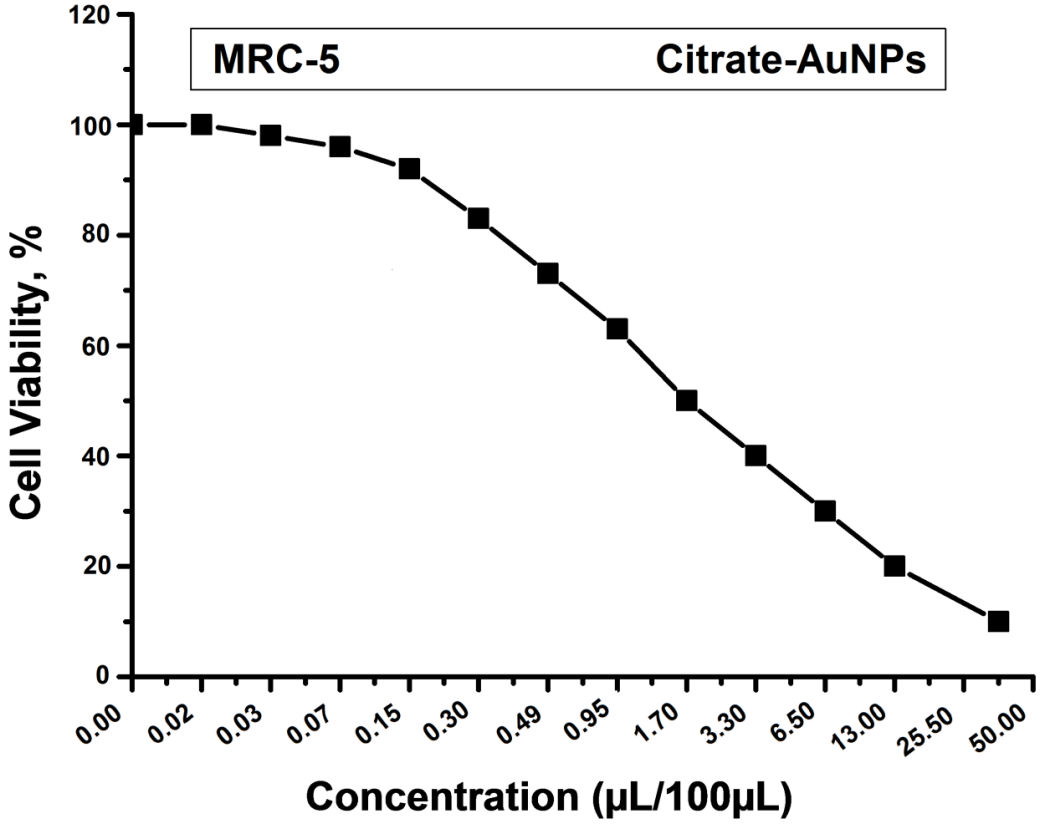

Fig. 5: Inhibitory cytotoxic activity against normal human lung fibroblast cells in different concentrations of citrate-AuNPs.

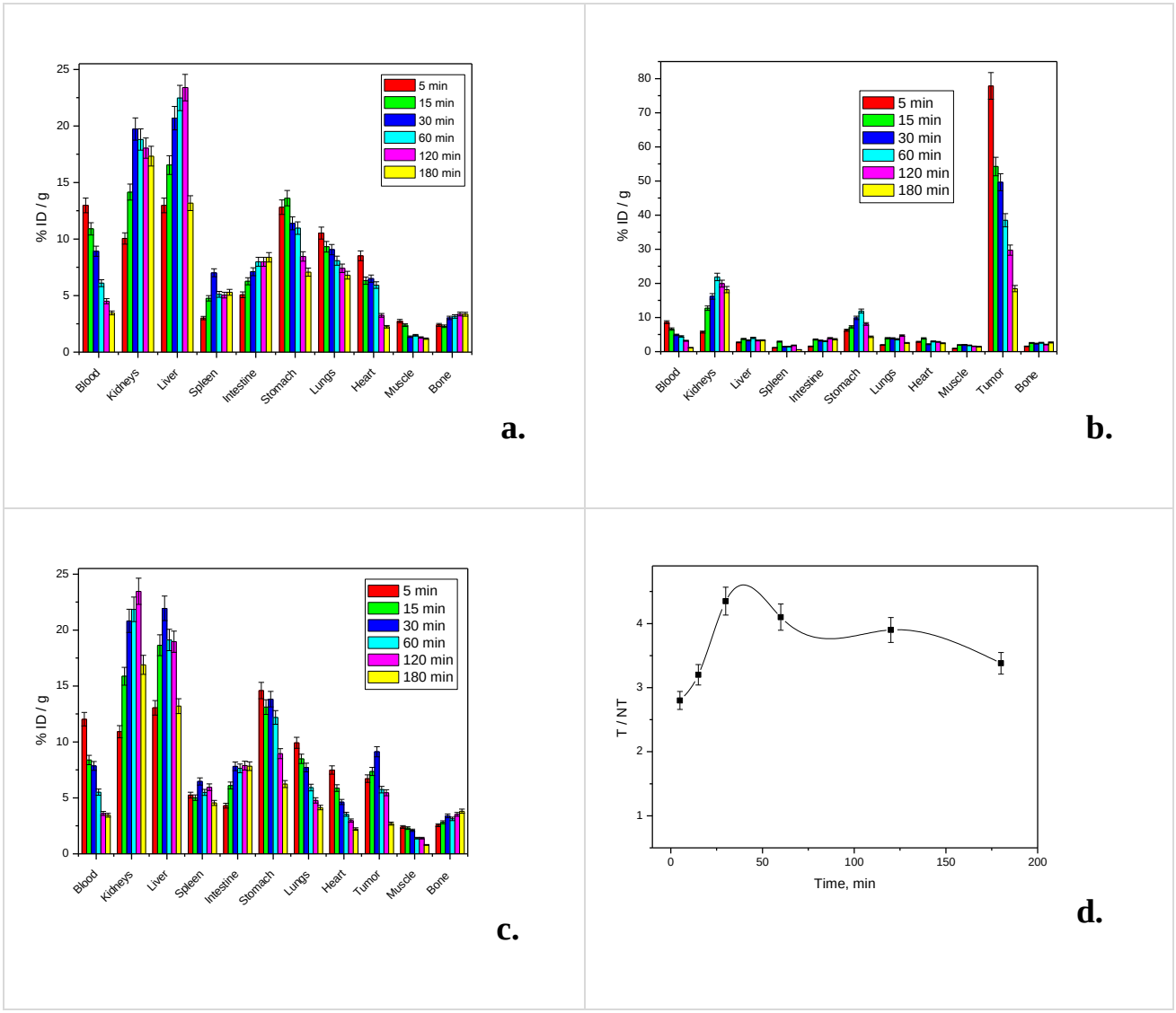

Fig. 6: Biodistribution of [^{99m}Tc]Tc-citrate-AuNPs: **a-** I.V. injection in normal Albino mice, **b-** I.T. injection in solid tumor bearing Albino mice, **c-** I.V. injection in solid tumor bearing Albino mice, **d-** T/NT ratio (calculated *via* I.V. injection in solid tumor bearing Albino mice).

Discussion

Citrate-AuNPs were synthesized according to Turkevich method [18] in which citrate salt initially acts as a reducing agent to reduce the Au^{3+} to Au^{0} and also acts as a stabilizing agent by forming a layer of citrate ions on the surface of formed gold nanoparticles. The appearance of the final deep wine red colour indicates the formation of colloidal gold nanoparticles with a spherical shape [19]. Both hydrodynamic diameter (21.4 nm) and core size diameter (10 nm) indicates that the formed nanoparticles were in a suitable nanoscale for biodistribution studies. The measured zeta potential (-11.8 mV) indicates the stability of the suspension.

Technetium-99m was bound to the nanoparticles during a complexation of the technetium-99m with the citrate on the surface of the gold nanoparticles. Stannous ions were used in most technetium radiopharmaceutical kits to reduce technetium from 7 to the desired oxidation state [20]. At low concentration of Sn(II) of 2 µg the labelling yield was low (69.3 %) because the amount of Sn(II) was insufficient to reduce all pertechnetate that found in the solution so the free pertechnetate was high (27.7 %); but at higher amounts of Sn(II) content over 10 µg, the labeling yield was decreased and reached to 76.3 % at 20 µg due to the formation of reduced hydrolyzed technetium colloid [21].

The pH is a crucial factor in labeling process. The pH of the reaction mixture must range from 6 to 8 to achieve convenient reduction and not affect the sensitive structures of nanoparticles [22]. At pH below or above the optimum value, the labeling yield was decreased (at pH 6 and 10 the labeling yield were 77.5 and 68.5 %, respectively) due to the formation of reduced hydrolyzed technetium colloid which is the main radiochemical impurity [23]. The content of citrate-AuNPs was also affecting the percent of labeling yield, the lower substrate amounts, the lower labeling yield due to its insufficient chelation with all

the reduced ^{99m}Tc species [24]. Further increase in the citrate-AuNPs amount has insignificant changes in the labeling yield. *In-vitro* stability of the formed complex was studied in order to determine the optimum time for biodistribution studies to avoid the formation of the undesired products which may be accumulated in the non-target organs; this stability was remained from 20 min up to 6h.

Physiological stability study in both serum and saline gave the same data and showed good stability. The resulted good stability at room temperature and also good physiological stability were very convenient for biological studies.

For cytotoxicity study, the number of the viable cells was not affected by addition of low concentrations of citrate-AuNPs (IC_{50} equal 1.7 µl/100 µl), so citrate-AuNPs can be used as a safe drug delivery system.

The *in-vivo* studies showed a high accumulation in liver, spleen and lungs which may be due to the accumulation of nanoparticles in reticuloendothelial system (RES) [25]. The accumulation of citrate-AuNPs in tumor tissues was attained by two routes: i) directly by the effect of citrate which can accumulate in cancer cells. ii) passively due to the enhanced permeability and retention effect (EPR) [26]. When citrate-AuNPs delivered by direct injection at the tumor site (group B), it is noticeable that citrate-AuNPs were retained inside the tumor site with a high ratio (more than 50 % after 30 min). This higher uptake in tumor tissues was preferable than many of recently developed agents such as: [^{99m}Tc]Tc-dendrimer-glutamine conjugate (2.86 at 2 h) [27], [^{99m}Tc]Tc-N-MAG-AMCPP (1.83 at 1 h) [28], [^{99m}Tc]Tc-DMSAme (2.49 at 2 h) [29] and [^{99m}Tc]Tc-sunitinib (3 at 1 h) [30].The behavior of citrate-AuNPs after systemic administration in solid tumor bearing mice (group C) showed that tumor tissues had gained radioactivity more than normal tissues. The promising results obtained throughout all the experimental time points in both B and C groups declared that citrate-AuNPs can be used as a new potential nano-sized radiopharmaceutical for tumor imaging.

Conclusion

A new radio nano-platform [^{99m}Tc]Tc-citrate-AuNPs was well synthesized with low hazard effects through green nanotechnology, which act as a target for tumor site with accumulation ratio reached to 4.35 as T/NT. [^{99m}Tc]Tc-citrate-AuNPs can also be retained inside tumor tissues *via* I.T. injection with a ratio more than 50 % after 30 min. These *in-vivo* studies indicate that [^{99m}Tc]Tc-citrate-AuNPs may be a good candidate for solid tumor imaging after preclinical studies.

References

1) **Mansoori, G. A., Mohazzabi, B., McCormack, B. and Jabbari, S. (2007).** Nanotechnology in cancer prevention, detection and treatment: bright future lies ahead. WRSTSD., **4:** 226-257.
2) **Maughan, C. N., Preston, S. G. and Williams, G. R. (2015).** Particulate inorganic adjuvants: Recent developments and future outlook. J. Pharm. Pharmacol., **67:** 426-449.
3) **Sutradhar, K. B. and Amin, M. dL. (2014).** Nanotechnology in Cancer Drug Delivery and Selective Targeting. ISRN Nanotechnology, 1-12.
4) **Assadi, M., Afrasiabi, K., Nabipour, I. and Seyedabadi, M. (2011).** Nanotechnology and nuclear medicine; research and preclinical applications. Hell J. Nucl. Med., **14:** 149-159.
5) **Makhsin, S. R., Teoh, P. L. and Razak, K. A. (2015).** Synthesis of Gold Nanoparticles and Its Conjugation Strategies to Biomolecules for Biomedical Applications. Rev. Adv. Sci. Eng., **4:** 3-21
6) **Katti, K. V., Khoobchandani, M., Thipe, V. C., AlYasiri, A. Y., Katti, K. K., Loyalkat, S. K., Sakr, T. M. and Lugao, B. (2018).** Prostate tumor therapy advances in nuclear medicine: green nanotechnology toward the design of tumor specific radioactive gold nanoparticles. J. Radioanal. Nucl. Chem., **318:** 1737-1747.
7) **Bhosale, R. R., Kulkarni, A. S., Gilda, S. S., Aloorkar, N. H., Osmani, R. A. and Harkare, B. R. (2014).** Innovative Eco-friendly Approaches for Green Synthesis of Silver Nanoparticles. Int. J. Pharm. Sci. Nanotech., **7:** 2328-2337.
8) **Mycielska, M. E., Patel, A., Rizaner, N., Mazurek, M. P., Keun, H., Patel, A., Ganapathy, V. and Djamgoz, M. B. A. (2009).** Citrate transport and metabolism in mammalian cells (Prostate epithelial cells and prostate cancer). Bio. Essays., **31:** 10-20.
9) **Philippe, I. and Hubert, L. (2016).** The reduced concentration of citrate in cancer cells: An indicator of cancer aggressiveness and a possible therapeutic target. Drug Resist. Updat., **29:** 47-53.
10) **Ren, J. G., Seth, P., Ye, H., Guo, K., Hanai, J. I., Husain, Z. and Sukhatme, V. P. (2017).** Citrate Suppresses Tumor Growth in Multiple Models through Inhibition of Glycolysis, the Tricarboxylic Acid Cycle and the IGF-1R Pathway. Sci. Rep., **7:** 4537.
11) **Xing, Y., Zhao, J., Conti, P. S. and Chen, K. (2014).** Radiolabeled Nanoparticles for Multimodality Tumor Imaging. Theranostics, **4:** 290-306.
12) **Key, J. and Leary, J. F. (2014).** Nanoparticles for multimodal in vivo imaging in nanomedicine. Int. J. Nanomedicine, **9:** 711-726.
13) **Xing, Y., Zhu, J., Zhao, L., Xiong, Z., Li, Y., Wu, S., Chand, G., Shi, X. and Zhao, J. (2018).** SPECT/CT imaging of chemotherapy-induced tumor apoptosis using 99mTc-labeled dendrimer-entrapped gold nanoparticles. Drug Deliv., **25:** 1384-1393.
14) **Salvanou, E. A., Bouziotis, P. and Tsoukalas, C. (2018).** Radiolabeled Nanoparticles in Nuclear Oncology. Advanced Nano Research, **1:** 38-55

15) **Essa, B. M., Sakr, T. M., Khedr, M. A., El-Essawy, F. A. and El-Mohty, A. A. (2015).** ^{99m}Tc-amitrole as a novel selective imaging probe for solid tumor: In silico and preclinical pharmacological study. Eur. J. Pharm. Sci., **76:** 102-109.

16) **Nasr, T., Bondock, S., Rashed, H. M., Fayad, W., Youns, M. and Sakr, T. M. (2018).** Novel hydrazide-hydrazone and amide substituted coumarin derivatives: Synthesis, cytotoxicity screening, microarray, radiolabeling and in vivo pharmacokinetic studies. Eur. J. Med. Chem., **151:** 723-739.

17) **Mohamed, K. O., Nissan, Y. M., El-Malah, A. A., Ahmed, W. A., Ibrahim, D. M., Sakr, T. M. and Motaleb, M. A. (2017).** Design, synthesis and biological evaluation of some novel sulfonamide derivatives as apoptosis inducers. Eur. J. Med. Chem., **135:** 424-433.

18) **Turkevich, J., Steverson, P. C. and Hillier, J. (1951).** A study of the nucleation and growth processes in the synthesis of colloidal gold. Discuss. Faraday Soc., **11:** 55-75.

19) **El-Nour, K. M. A., Salam, E. T. A., Soliman, H. M. and Orabi, A. S. (2017).** Gold Nanoparticles as a Direct and Rapid Sensor for Sensitive Analytical Detection of Biogenic Amines. Nanoscale Res. Lett., **12:** 231.

20) **Motaleb, M. A., Selim, A. A., El-Tawoosy, M., Sanad, M. H. and El-Hashash, M. A. (2017).** Synthesis, radiolabeling and biological distribution of a new dioxime derivative as a potential tumor imaging agent. Radioanal. Nucl. Chem., **314:** 1517-1522.

21) **Sakr, T. M., Essa, B. M., El-Essawy, F. A. and El-Mohty, A. A. (2014).** Synthesis and Biodistribution of ^{99m}Tc-PyDA as a Potential Marker for Tumor Hypoxia Imaging. Radiochemistry, **56:** 76-80.

22) **Psimadasa, D., Bouziotisb, P., Georgouliasa, P., Valotassioua, V., Tsotakosb, T. and Loudos, G. (2013).** Radiolabeling approaches of nanoparticles with ^{99m}Tc. Contrast Media Mol. Imaging, **8:** 333-339.

23) **Motaleb, M. A., Selim, A. A., El-Tawoosy, M., Sanad, M. H. and El-Hashash, M. A. (2018).** Synthesis, characterization, radiolabeling and biodistribution of a novel cyclohexane dioxime derivative as a potential candidate for tumor imaging. Int. J. Radiat. Biol., **94:** 590-596.

24) **Al-Wabli, R. I., Sakr, T. M., Khedr, M. A., Selim, A. A., Motaleb, M. A. and Zaghary, W. A. (2016).** Platelet-12 lipoxygenase targeting via a newly synthesized curcumin derivative radiolabeled with technetium-99m. Chem. Cent. J., **10:** 73-84.

25) **Garnett, M. C. and Kallinteri, P. (2006).** Nanomedicines and nanotoxicology: some physiological principles. Occup. Med., **56:** 307-311 .

26) **Nakamura, Y., Mochida, A., Choyke, P. L. and Kobayashi, H. (2016).** Nanodrug Delivery: Is the Enhanced Permeability and Retention Effect Sufficient for Curing Cancer? Bioconjug. Chem., **27:** 2225-2238.

27) **Ghoreishi, S. M., Khalaj, A., Sabzevari, O., Badrzadeh, L., Mohammadzadeh, P., Motlagh, S. S. M., BitarafanRajabi, A. and Ardestani, M. S. (2018).** Technetium-99m chelator-free radiolabeling of specific glutamine tumor imaging nanoprobe: *in vitro* and *in vivo* evaluations. Int. J. Nanomedicine, **13:** 4671-4683.

28) **Ding, R., He, Y., Xu, J., Liu, H., Wang, X., Feng, M., Qi, C., Zhang, J. and Peng, C. (2012).** Preparation and bioevaluation of ^{99m}Tc nitrido radiopharmaceuticals with pyrazolo [1,5-a] pyrimidine as tumor imaging agents. Med. Chem. Res., **21:** 523-530.

29) **Zhang, J., Yu, Q., Huo, J., Pang, Y., Yang, S., He, Y., Tang, T., Yang, C. and Wang, X. (2010).** Synthesis and biodistribution of a novel ^{99m}Tc-DMSA-metronidazole ester as a potential tumor hypoxia imaging agent. J. Radioanal. Nucl. Chem., **283:** 481-485.

30) **Sakr, T. M., El-Safoury, D. M., Awad, G. A. S. and Motaleb, M. A. (2013).** Biodistribution of ^{99m}Tc-sunitinib as a potential radiotracer for tumor hypoxia imaging. J. Label Compd. Radiopharm., **56:** 392-395.